DYNAMIC SIMULATION OF A HIGH PRESSURE REGULATOR

A. R. Shahani*, H. Esmaili, A. Aryaei, S. Mohammadi and M. Najar
Department of Applied Mechanics, Faculty of Mechanical Engineering, K. N. Toosi University of Technology, Pardis Street, Mollasadra Avenue, Vanak Square, P.O. Box 19395-1999, Tehran, Iran

Received: 3/7/2011 Accepted: 29/8/2011 Online: 11/9/2011

ABSTRACT
In this paper, the dynamic simulation for a high pressure regulator is performed to obtain the regulator behavior. To analyze the regulator performance, the equation of motion for inner parts, the continuity equation for diverse chambers and the equation for mass flow rate were derived. Because of nonlinearity and coupling, these equations are solved using numerical methods and the results are presented. Additionally, the dynamic analysis results consist of the output pressure change versus time, the displacement of the moving parts versus time, the regulator mass flow rate versus time and the output pressure versus mass flow rate in different controlling spring pre-loads. Furthermore, the sensitivity analysis is carried out and the main parameters affecting the regulator performance are identified. Finally, the results of the dynamic simulation are validated by comparing them with the experimental results.

KEYWORDS: High pressure regulator, Dynamic analysis, Non-linear analysis, Numerical method

INTRODUCTION

The many remarkable characteristics of pneumatic systems such as energy-saving, simple structure and operation, high efficiency and suitability for working in harsh environments, has led to their wide use for many years in different industries such as petroleum and aerospace engineering [1,2]. Particularly, gas pressure regulators are widely used in diverse applications to control the operational pressure of the gas. Gas regulators are devices that maintain constant output pressure regardless of the variations in the input pressure. They range from simple, single stage [3,4] to more complex, multi stage regulators [5,6], but the principle of operation is the same in all of them [7].]. Limited research is published on pressure regulators, due to concerns over proprietary information. It should be pointed out that, for many years, the trial-and-error method of developing various kinds of pressure regulators was the only accepted way. Most probably, this was the result of the inherent difficulties in the modeling of these regulators. The difficulties encountered in making a dynamic analysis of the gas regulator are largely due to the nonlinearities of the equations describing the regulator. Tsai and Cassidy [8] introduced, probably for the first time, a systematic analysis, linear as well as nonlinear for

* To whom correspondence should be addressed. E-mail: shahani@kntu.ac.ir.

a simple pressure regulator. Dustin [9] presented an analog simulation of spring loaded, direct acting, single stage gas pressure regulator. The simulation was based on a pressure regulator used in a space power generator. In this investigation, the effects of regulator design parameters on stability, transient response and steady state accuracy were examined. Kakulka et al. [10] studied the piston pressure-sensing unit regulator that had a conical poppet valve for regulating the gas flow. The dynamic effects of restrictive orifices and the upstream and downstream volumes were addressed in the modeling and analysis. Zafer et al. [11] developed a comprehensive dynamic model for a gas pressure regulator in order to gain a better understanding of its behavior. They first modeled an existing regulator and used empirical data as necessary to identify parameter values for the model. Using a linearized version of the mentioned model, they investigated the effects of parameter variations using classical root-locus technique. Indeed, their main work was to identify the most influential system parameters on the stability of the system.

Several studies were carried out in order to characterize the behavior of natural gas regulators [12-14]. More recently, Rami et al. [15] developed a methodology and library of models to study the stability of any type of natural gas pressure regulator as an industry-oriented project. Their results were also validated by experiments. Additionally, they investigated the effects of operating conditions and installations on the stability of the pressure regulator in another paper [16].

Another mathematical model developed for a newly designed pressure regulator was built by Nabi et al. [17]. They obtained the complete dynamic model and its simulated response contributed considerably to the understanding of different effects influencing actual regulator behavior. Using a numerical solution, based on Runge-Kutta method, the regulator performance was studied. Finally, some tests were performed to verify the physical model.

To the best knowledge of the authors, a complete dynamic model especially for high pressure regulators which works on more than 300 bars has not been presented yet. In this paper the dynamic simulation of a high pressure regulator has been presented. The continuity equations have been written for the main chambers of the regulator. The general mass flow rate of the regulator is controlled by a moving spool the relative position of which with respect to the body of the chamber (x) determines the amount of passing flow. In fact, the spool-body pair, which designate the passage ‘x’, act like a converging nozzle for which we can write the nozzle equation of mass flow. The third set of equations is the dynamic equation of motion of the spool and other parts moving with it. These non-linear equations are solved numerically to determine the performance of the air regulator valve. The results of the simulation have been verified by comparing them with the experimental results. Finally a sensitivity analysis is carried out to determine the most influential parameters on the performance of the valve. This is an important result from the design and fabrication point of view which designates which elements must be designed and fabricated more carefully.

REGULATOR OPERATION AND DESCRIPTION

In Fig. (1), the schematic sketch of the pressure regulator is presented. The first element of the regulator that affects the pressurized air is the air filter. The filter acts like an air pressure resistance and it causes a little drop in pressure. The main role of the filter is to prevent the entrance of any contaminants based on the related standards [18].

Other parts are a little spring and a slipper pushing against it. Air flows through the cylindrical area and arrives at the spool entrance. Indeed, the slipper plays one of the main controlling roles in the air regulator and with changing the distance between this element and the spool guide, the resistance of this section is changed and despite variable input pressure, the pressure remains constant in the output port. The spool pushes a controlling spring with large stiffness in the top section of the pressure regulator. This spring plays an important role in indicating the output pressure magnitude. It is clear that the output pressure has direct relation with the spring preload. In the other words, with increase in the preload of the controlling spring by turning the regulating bolt, the output pressure will increase. Additionally, it is worth noting that the little spring below the slipper always pushes it up. In this way,

all of the moving parts of the regulator are in touch together during the regulator operation. Owing to this point, the mentioned pressure regulator is a single degree of freedom system. Another noticeable point is that the pneumatic systems are very sensitive and precise and a little change in chamber volume will result in extreme changes in the output pressure.

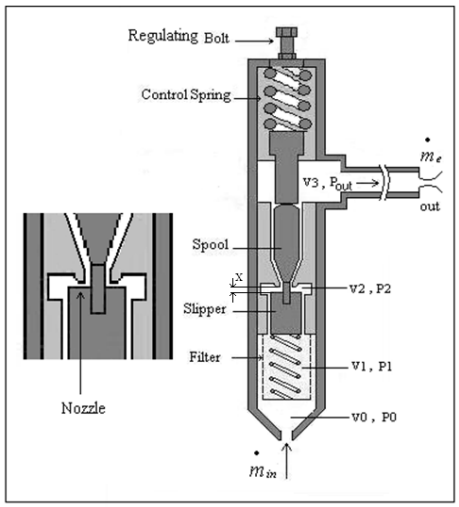

Fig. 1. Schematic view of the gas pressure regulator.

ANALYSIS AND MODELING OF THE HIGH PRESSURE REGULATOR

According to Fig. (1), the inner moving parts are: the slipper, the spring below the slipper, the spool, the piston and the controlling spring. As the input port is opened and the air enters the different ducts, the pressure in the chambers V_0, V_1, V_2, V_3 increases. By increasing P_{out} in the chamber V_3, the piston which is located below the controlling spring moves up. The large force exerted by the controlling spring on the spool, slipper and piston causes the valve to act as a one degree freedom system. When the spool moves toward further compressing the controlling spring, the slipper moves up as a result and the nozzle duct of the regulator becomes smaller. This process continues until the forces which result from the pressure acting on different surfaces of the inner moving parts become equal to the force exerted from the controlling spring. When the input pressure increases, the slipper moves up and the nozzle duct becomes smaller causing the mass flow rate passing through the nozzle and the output pressure of the regulator to remain constant. In addition, by decreasing the input pressure, the slipper moves down and opens the nozzle duct. Hence, the mass flow rate and the output pressure remain constant due to the decrease in fluid resistance.

In this section, after explaining the assumptions which are considered in modeling and analysis, the governing equations such as the continuity equation for the chamber located after the spool, the orifice equation and the dynamic equation of the moving parts of the regulator are described.

Assumptions

The presented modeling and analysis is based on the following assumptions:

1. Generally, the moving inner parts act like a single unit. This assumption can be made because all parts are in touch during the action of the valve. Assuming a single unified movement for these internal parts reduces the dynamic equation to that of a single degree of freedom system.
2. The adiabatic process is occurring in the pressure regulator. This is reasonable because of the short time response compared to the heat-transfer process time.

3. The gas behaves ideally and ideal gas equation can be used in the simulation.
4. The gas pressure and density in different chambers are assumed to be homogenous. In this way, a unique property is used for a specific chamber.
5. The air leakage is negligible compared to the input mass flow rate. Hence, it is neglected.
6. The seals of the regulator may produce a constant coulomb friction force, acting in the opposite direction of the motion.

The Dynamic Equations for Pressure and Temperature

In this section, the dynamic equations for pressure and temperature are derived based on the mass and energy balances [17]. For a variable control volume with single input and single output flows these equations are expressed as:

$$\frac{dP}{dt} = \frac{R\ \gamma}{V}(T_{in}\ \dot{m}_{in} - T\ \dot{m}_{out}) - \frac{\gamma\ AP}{V}\dot{x} \tag{1}$$

$$\frac{dT}{dt} = \frac{RT^2}{V\ P}[(\gamma\frac{T_{in}}{T} - 1)\dot{m}_{in} - (\gamma - 1)\dot{m}_{out}] - \frac{(\gamma - 1)AT}{V}\dot{x} \tag{2}$$

where the subscripts in and out denotes input and output properties, respectively and γ is the gas specific heat ratio.

For constant volume V_0 (Fig. (1)) we have $\dot{x} = 0$ and thus the above equations are reduced to:

$$\frac{dP_0}{dt} = \frac{R\ \gamma}{V_0}(T_{in}\ \dot{m}_{in} - T_0\ \dot{m}_1) \tag{3}$$

$$\frac{dT_0}{dt} = \frac{R\ T_0^{\ 2}}{V_0\ P_0}[(\gamma\frac{T_{in}}{T_0} - 1)\dot{m}_{in} - (\gamma - 1)\dot{m}_1] \tag{4}$$

where $\dot{m}_1$ is the mass flow rate flowing through the filter. According to Fig. (1), for the chamber V_1 having variable volume, the corresponding pressure and the temperature equations are:

$$\frac{dP_1}{dt} = \frac{R\ \gamma}{V_1}(T_0\ \dot{m}_1 - T_1\ \dot{m}_2) - \frac{\gamma\ A_1P_1}{V_1}\dot{x} \tag{5}$$

$$\frac{dT_1}{dt} = \frac{RT_1^{\ 2}}{V_1P_1}[(\gamma\frac{T_0}{T_1} - 1)\dot{m}_1 - (\gamma - 1)\dot{m}_2] - \frac{(\gamma - 1)A_1T_1}{V_1}\dot{x} \tag{6}$$

In these equations, $\dot{x}$ is the time derivation of the slipper displacement or the slipper velocity, A_1 is the area of the slipper and $\dot{m}_2$ is the mass flow rate passing through the slipper. In the same way, for the chamber V_2, the pressure and the temperature equations can be written as:

$$\frac{dP_2}{dt} = \frac{R\ \gamma}{V_2}(T_1\ \dot{m}_2 - T_2\ \dot{m}_s) + \frac{\gamma\ A_2P_2}{V_2}\dot{x} \tag{7}$$

$$\frac{dT_2}{dt} = \frac{RT_2^{\ 2}}{V_2P_2}[(\gamma\frac{T_1}{T_2} - 1)\dot{m}_2 - (\gamma - 1)\dot{m}_s] + \frac{(\gamma - 1)A_2T_2}{V_2}\dot{x} \tag{8}$$

where A_2 is the area of the other side of the slipper and $\dot{m}_s$ is the mass flow rate passing through the upper surface of the slipper. Because the volume of the chamber increases with increase in x, the coefficient of $\dot{x}$ will be positive in the above equation.
Finally, for the chamber V_3, the pressure and the temperature equations can be expressed as:

$$\frac{dP_{out}}{dt} = \frac{R\ \gamma}{V_3}(T_2\ \dot{m}_s - T_{out}\ \dot{m}_e) - \frac{\gamma\ A_3 P_{out}}{V_3}\dot{x} \tag{9}$$

$$\frac{dT_{out}}{dt} = \frac{RT_{out}^{\ 2}}{V_3 P_{out}}[(\gamma\frac{T_2}{T_{out}} - 1)\dot{m}_s - (\gamma - 1)\dot{m}_e] - \frac{(\gamma - 1)A_3 T_{out}}{V_3}\dot{x} \tag{10}$$

where A_3 is the piston area located at the bottom of the control spring (sensing area) and $\dot{m}_e$ is the mass flow rate passing through the output nozzle.

The Orifice Flow Equation in Regulator Ducts
The relation for the mass flow rate of the air in the regulator entrance duct is:

$$\dot{m}_{in} = c_{din} S_{in} (\frac{2}{\gamma + 1})^{\frac{1}{\gamma - 1}} \sqrt{\frac{2\gamma}{\gamma + 1}\frac{1}{RT_{in}}}\ P_{in} \tag{11}$$

$$\dot{m}_{in} = c_{din} S_{in} \sqrt{\frac{2\gamma}{\gamma - 1}\frac{1}{RT_{in}}}\ P_{in} \sqrt{[(\frac{P_0}{P_{in}})^{\frac{2}{\gamma}} - (\frac{P_0}{P_{in}})^{\frac{\gamma+1}{\gamma}}]} \tag{12}$$

Eqs. (11) and (12) are used when $\frac{P_0}{P_{in}} < 0.528$ and $\frac{P_0}{P_{in}} > 0.528$, respectively [19]. In these equations, c_{din} is the discharge coefficient and is assumed to be 1 [20]. S_{in} is the orifice area which is constant. Similarly, the mass which flows through the filter and the mass flow rate passing through the nozzle can be written using Eqs. (11) and (12). The mentioned nozzle is located above the slipper and is shown in Fig. (1). In this nozzle the orifice area (S_s) changes with the spool position (x) variation:

$$S_s = w\ (x_0 - x) \tag{13}$$

where w is the area gradient [2]. Finally, the mass flow rate through regulator output nozzle can be found through the use of Eqs. (11) and (12).

Equation of Motion of the Moving Parts
The position of the moving parts especially the spool, which determines the output pressure of the regulator, can be extracted by solving the differential equation of the motion. Fig. (2) shows the free-body diagram of the moving parts of the regulator.
Based on one degree of freedom system, the equation of motion can be written as:

$$M\ddot{x} + F_c\, sign(\dot{x}) + Kx = A_1 P_1 - A_2 P_2 + A_3 P_{out} - F_0 \tag{14}$$

where M is the total mass of the moving elements plus one third of the mass of the spring. K is the spring stiffness, F_0 is the spring pre-compression force, F_c is the friction force which resulted from the dry friction between the seal and the body and can be calculated as:

$$F_c = \mu P_{out} A_p \tag{15}$$

in which μ and A_p are the friction coefficient and the area between packing and its supporter, respectively. Regarding equations of motion, it can be easily seen that the derived equations are nonlinear and coupled. So, the equations have to be solved numerically.
In the stable condition, the force resulted from the output pressure is in equilibrium with the spring force which specifies the position of the spool and as a result the required area for the nozzle. By changing the spring preload, the volume flow rate, output pressure of regulator changes, too.

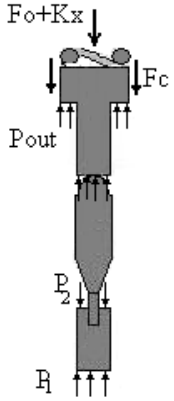

Fig. 2. Free body diagram of internal parts.

EXPERIMENTAL SETUP
Fig. (3) shows the schematic view of the experimental set up for testing the pressure regulator. To investigate the output pressure of the regulator, two pressure gauges were installed both at the input and output ports.

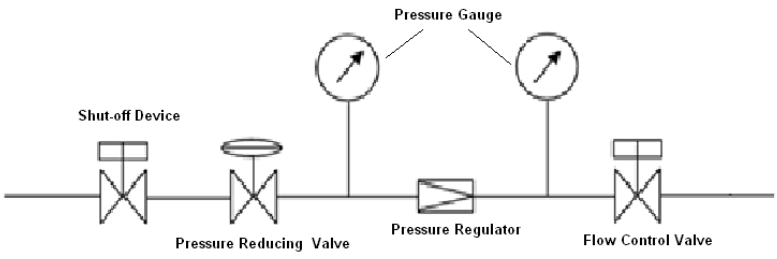

Fig. 3. Pneumatic circuit for conducting experiments.

SENSITIVITY ANALYSIS

In this part, the sensitivity analysis for different important parameters of the pressure regulator is performed. The obtained equations are non-linear and the output pressure cannot be expressed as explicit function of the regulator's main parameters, therefore, the sensitivity analysis is done using numerical methods. In this way, by changing one specific parameter when other parameters are constant, the output pressure sensitivity versus the specific parameter is obtained.

It is worth noting that the value of the sensitivity parameter can be negative, positive or zero. The desired value for sensitivity should be near to zero. In other words, the output pressure should not have a remarkable variation when the specific parameter varies.

It is possible that some pneumatic components are not precisely designed and manufactured. The sensitivity analysis is performed in order to detect the parameters that have noticeable effects on the output pressure.

Sensitivity Analysis with Respect to Control Spring Stiffness (K)

Several parameters may affect the stiffness of the control spring. Material considerations, change in properties due to, for example, relaxation and creep, and also manufacturing limitations could change the spring stiffness. So, the effects of the stiffness change on the output pressure should be investigated. The output sensitivity with respect to the control spring stiffness can be expressed as:

$$S_K^{P_{out}} = \frac{K}{P_{out}} \frac{dP_{out}}{dK} \tag{16}$$

Sensitivity Analysis with Respect to the Area Gradient (w)

One of the most important parameters affecting the output pressure is the area gradient which controls the mass flow rate. The output sensitivity with respect to the area gradient may be defined as:

$$S_w^{P_{out}} = \frac{w}{P_{out}} \frac{dP_{out}}{dw} \tag{17}$$

Sensitivity Analysis with Respect to the Sensing Area (A_3)

The main area that is affected by the output pressure is the sensing area which is located at the bottom of the controlling spring. Therefore, any change in this area contributes to output pressure change. The output sensitivity with respect to the sensing area is:

$$S_{A_3}^{P_{out}} = \frac{A_3}{P_{out}} \frac{dP_{out}}{dA_3} \tag{18}$$

RESULTS AND DISCUSSIONS

In order to verify the simulation results, a test was conducted using the experimental set up of Fig. (3). The input pressure was gradually increased from zero to 180 bars. Fig. (4) shows the results of the simulation compared with the experimental data in the steady state condition. Based on this figure an increase in the input pressure, will result in an increase in the output pressure. When the input pressure reaches 120 bars, the output pressure reaches a specified value and remains constant afterwards. By further increasing the input pressure, there is no change in the magnitude of the output pressure. Actually this is the "regulated value" of the output pressure. As it can be seen, there is a good agreement between the simulation and test results.

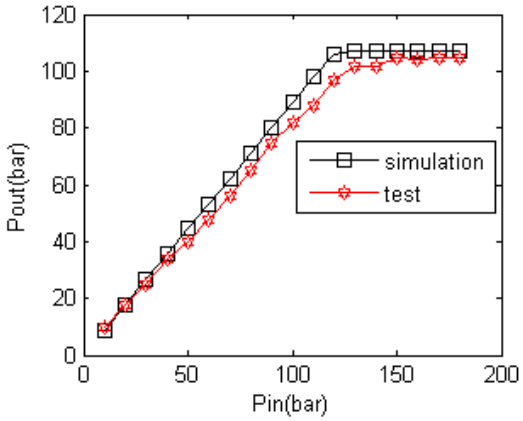

Fig. 4. Comparison of simulation and test results for the pressure regulator.

Fig. (5) shows the time response of the regulator for two different chamber volumes (V3). It is seen that as the volume chamber V3 increases, the time constant of the valve also increases while the oscillations about the "regulated pressure" decreases.

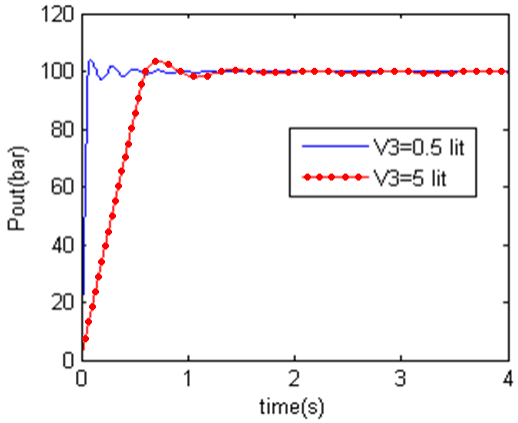

Fig. 5. Output pressure versus time for two different chamber volumes.

Additionally, Fig. (6) represents the spool displacement with respect to time. The real time delay of the valve is very small, but the chamber volume after the spool (V3) was exaggerated to show its effect on the overshoot and time delay of the valve response. It is seen from the figure that there is a settle time step in which the spool remains undisplaced. This is because of the capacity of the chamber volume and the time required that this volume is filled.

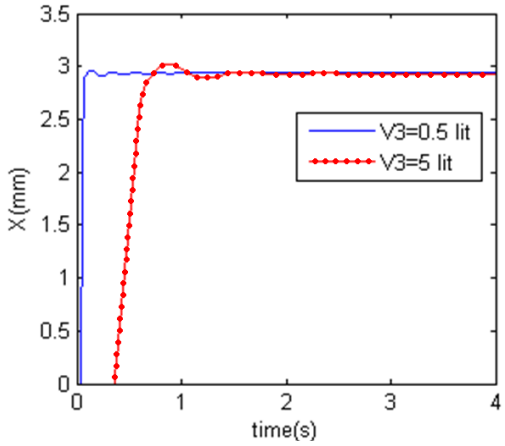

Fig. 6. The spool displacement versus time.

The effect of the spring pre-load on the regulator performance is shown in Fig. (7). It is observed that as the spring preload increases via tightening the regulating bolt, the output pressure increases proportionally.

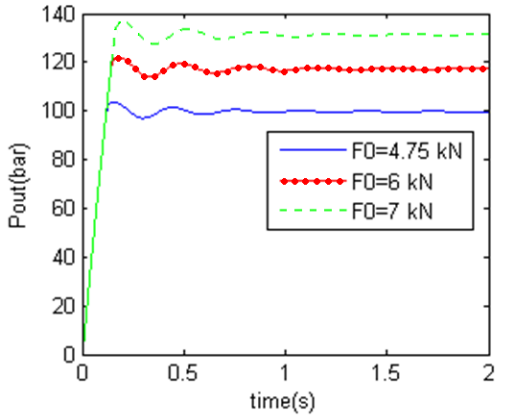

Fig.7. The output pressure variation with respect to time.

Also, the variations of mass flow rate passing through the output port is shown in Fig. (8). As is observed, the mass flow rate increases until it reaches a steady state value.

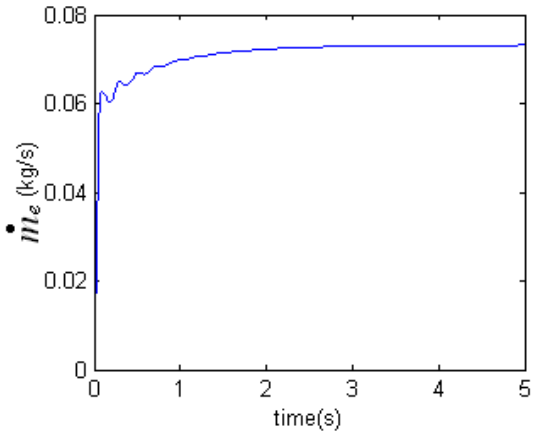

Fig. 8. Mass flow rate passing through the output port.

In the last part of this section, the sensitivity analysis results are presented. The output pressure sensitivity with respect to the controlling spring stiffness is shown in Fig. (9). The output pressure sensitivity decreases by increasing the spring stiffness. For instance, the sensitivity in $K = 1000\,(N/mm)$ is 1.048. In the other words, when the stiffness increases 1%, the output pressure variation is about 1.048% which is considerable.

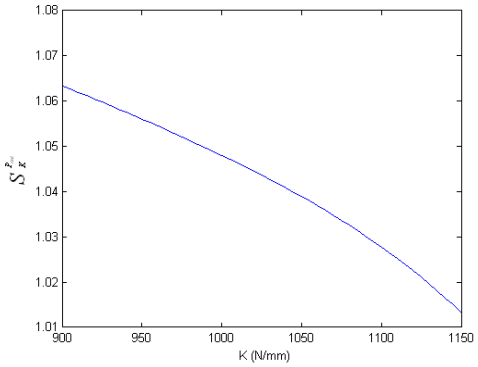

Fig. 9. The output pressure sensitivity with respect to the controlling spring stiffness.

Similarly, Figs. (10) and (11) show the output pressure sensitivity with respect to the area gradient (w) and the sensing area (A_3), respectively.

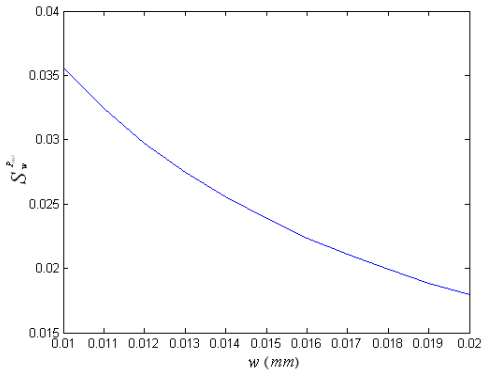

Fig. 10. The output pressure sensitivity with respect to the area gradient.

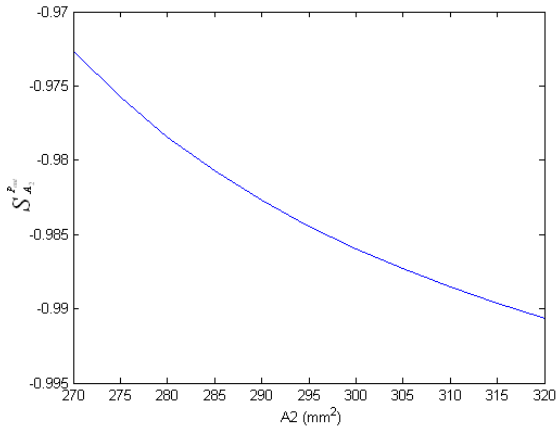

Fig. 11. The output pressure sensitivity with respect to the sensing area.

It is seen that the parameter (w) has little effect on the output pressure of the valve. This is desirable because it represents that an unwanted change in the diameter of the spool area (which can occur due to fabrication problems) has no important effect on the valve performance. Fig. (11) shows that an increase in the sensing area (A_3) causes a considerable decrease in the output pressure. Hence, the control spring plays an important role in the regulator performance, so, it should be accurately designed and manufactured.

CONCLUSIONS

Dynamic simulation of a high pressure regulator was accomplished. For this purpose, three sets of conservation equations consisting of the continuity equations, the orifice mass flow rate equations and the equation of motion have been extracted and the resultant nonlinear equations have been solved. For the sake of verification of the simulation results, some experiments were conducted. The following results can be drawn from the performed analysis:

1- A very good agreement exists between the simulation and experimental results.

2- As the volume chamber V3 increases, the time constant of the valve also increases while the oscillations about the “regulated pressure” decreases.

3- By increasing the spring preload via tightening the regulating bolt, the output pressure increases proportionally.
4- According to the sensitivity analysis, two parameters that have an important effect on the output pressure of the regulator are the control spring stiffness and the sensing area (A_3). So, the control spring and the sensing area of the regulator should be designed and manufactured carefully. The demensions, material properties and mechanics should be taken into consideration.

REFERENCES

[1] J. Pu, P. R. Moore and C. B. Wong, "Smart Components-based Servo-pneumatic Actuation Systems", *Microprocessors and Microsystems*, Vol. 24, pp 113-119, (2000).
[2] H. E. Merrit, "*Hydraulic Control Systems*", John Wiley & Sons, New York, (1967).
[3] R. Mooney, "Pilot-Loaded Regulator: What You Need to Know", *Gas Industries*, pp 31-33, (1989).
[4] R. Brasilow, "The Basics of Gas Regulators", *Welding Design and Fabrication*, pp 61-65, (1989).
[5] A. Krigman, "*Guide to Selecting Pressure Regulators*", InTech, pp 51-65, (1984).
[6] E. Gill, "Air-loaded Regulators", *The Smart Control Valve Alternative*, InTech, pp 21-22, (1990).
[7] S.J. Bailey, "Pressure controls 1987: sensing art challenges old technologies", *Control Engineering* , pp 80-85, (1987).
[8] D. H. Tsai and E. C. Cassidy, "Dynamic Behavior of Simple Pneumatic Pressure Reducer", *ASME Journal of Basic Engineering*, Vol. 83, pp 253, (1961).
[9] M. O. Dustin, "Analog Computer Study of Design Parameter Effects on the Stability of a Direct Acting Gas Pressure Regulator", *NASA TN D-6267*, (1971).
[10] D.J. Kukulka, A. Benzoni and J.C. Mallendorf, "Digital Simulation of a Pneumatic Pressure Regulator", *Simulation, Modelling, Practice and Theory*, pp 252-266, (1994).
[11] N. Zafer and G. R. Luecke, "Stability of Gas Pressure Regulators", *Applied Mathematical Modelling*, Vol. 32, pp 61-82, (2008).
[12] Association Technique de l'Industrie et du Gaz en France. Manuel pour le transport et la distribution du gaz, titre V, de´tente et regulation du gaz, ISBN 2-8655-044-7, (1990).
[13] K. J. Adou, "*Etude Du Fonctionnement Dynamique des re´Gulateursdetendeurs Industriels de Gaz*", PhD Thesis, Universite´ de Paris VI; (1989).
[14] F. Favret, M. Jemmali, J. P. Cornil, F. Deneuve and J. P. Guiraud, "Stability of Distribution Network Governors", *R and D Forum Osaka Gas*; (1990).
[15] E. G. Rami, B. Jean Jacques, G. Pascal and M. Francois, "Stability Study and Modelling of a Pressure Regulating Station", *International Journal of Pressure Vessels and Piping*, Vol. 82, pp 51-60, (2005).
[16] E. G. Rami, B. Jean Jacques, D. Bruno and M. Francois, "Modelling of a Pressure Regulator", *International Journal of Pressure Vessels and Piping*, Vol. 84, pp 234-243, (2007).
[17] A. Nabi, E. Wacholder and J. Dayan, "Dynamic Model for a Dome-Loaded Pressure Regulator", *Transactions of ASME, Dynamic Systems, measurement, and Control*, Vol. 122, pp 290-297, (2000).
[18] International Standard, ISO 8573, Parts 1-7, Second Edition, (2001).
[19] Peter Beater, "*Pneumatic Drives"*, System Design, Modelling and Control, Springer, New York, (2007).
[20] Andersen, B.W., "*The analysis and Design of Pneumatic Systems*", John Wiley & Sons Pub., New York, USA, (1967).